THE JOURNAL OF BIOLOGICAL CHEMISTRY VOL. 286, NO. 3, pp. 1819–1827, January 21, 2011

Chymotrypsin C Is a Co-activator of Human Pancreatic Procarboxypeptidases A1 and A2*[S]

Received for publication, September 21, 2010, and in revised form, November 14, 2010 Published, JBC Papers in Press, November 22, 2010, DOI 10.1074/jbc.M110.187369

Richárd Szmola[‡1], Melinda Bence[‡1], Andrea Carpentieri[‡], András Szabó[‡], Catherine E. Costello[§], John Samuelson[‡], and Miklós Sahin-Tóth[‡2]

From the [‡]Department of Molecular and Cell Biology, Boston University Henry M. Goldman School of Dental Medicine, Boston, Massachusetts 02118 and the [§]Department of Biochemistry, Boston University School of Medicine, Boston, Massachusetts 02118

Human digestive carboxypeptidases CPA1, CPA2, and CPB1 are secreted by the pancreas as inactive proenzymes containing a 94–96-amino acid-long propeptide. Activation of procarboxypeptidases is initiated by proteolytic cleavage at the C-terminal end of the propeptide by trypsin. Here, we demonstrate that subsequent cleavage of the propeptide by chymotrypsin C (CTRC) induces a nearly 10-fold increase in the activity of trypsin-activated CPA1 and CPA2, whereas CPB1 activity is unaffected. Other human pancreatic proteases such as chymotrypsin B1, chymotrypsin B2, chymotrypsin-like enzyme-1, elastase 2A, elastase 3A, or elastase 3B are inactive or markedly less effective at promoting procarboxypeptidase activation. On the basis of these observations, we propose that CTRC is a physiological co-activator of proCPA1 and proCPA2. Furthermore, the results confirm and extend the notion that CTRC is a key regulator of digestive zymogen activation.

Chymotrypsin C (CTRC)[3] is a digestive protease synthesized and secreted by pancreatic acinar cells as an inactive precursor (chymotrypsinogen C), which becomes activated in the duodenum after trypsin cleaves the Arg^{29}–Val^{30} peptide bond at the C-terminal end of the propeptide. The severed propeptide remains attached to CTRC through a disulfide bond. CTRC exhibits chymotrypsin-like substrate specificity as it cleaves after Phe, Tyr, Leu, Met, Gln, and Asn amino acid residues (1–3), but CTRC shares higher sequence identity with pancreatic elastases than with chymotrypsins. CTRC is best distinguished from chymotrypsins A and B by its significantly higher activity on leucyl and glutaminyl peptide bonds (1–4). In the pancreatic juice of ruminants chymotrypsinogen C is found in ternary complex with procarboxypeptidase A (proCPA) and proproteinase E or in binary complex with proCPA (5–7).

Recently, we identified human CTRC as a specific regulator of activation and degradation of human cationic trypsinogen and trypsin (8, 9). Thus, CTRC stimulates autoactivation of cationic trypsinogen by processing the trypsinogen activation peptide to a shorter form that is more susceptible to tryptic activation. Mutation A16V, which changes the first amino acid in the trypsinogen activation peptide, accelerates CTRC-mediated processing, and carriers of this mutation are at risk of developing chronic pancreatitis (8). CTRC can also cleave the Leu^{81}–Glu^{82} peptide bond within the calcium binding loop of cationic trypsin, when calcium concentrations are low, and the binding loop is unoccupied. The combination of this cleavage and an autolytic cleavage at Arg^{122} results in the degradation and complete inactivation of cationic trypsin (9). CTRC-mediated trypsin degradation is inhibited by calcium, which at millimolar concentrations stabilizes the calcium binding loop. Genetic evidence suggests that trypsin degradation is an important protective mechanism in the pancreas, as loss-of-function variants of CTRC increase the risk for chronic pancreatitis (10, 11), and the trypsinogen mutation R122H, which blocks CTRC-facilitated trypsin degradation by eliminating the Arg^{122} autolysis site, causes hereditary pancreatitis (9, 12).

Compelled by these observations, we have initiated a systematic investigation into novel regulatory roles of CTRC in digestive enzyme activation and degradation. Here, we present studies on the function of CTRC in promoting activation of human proCPA1 and proCPA2. Pancreatic procarboxypeptidases are the precursors to digestive exopeptidases responsible for removal of C-terminal residues from their dietary protein and peptide substrates (13, 14). A-type carboxypeptidases (encoded by the CPA1 and CPA2 genes in humans) act on aromatic and aliphatic amino acid residues exposed by the action of chymotrypsins and elastases, whereas the B-type carboxypeptidase (encoded by the CPB1 gene) hydrolyzes C-terminal Lys and Arg residues generated by tryptic cleavages. Procarboxypeptidases contain a 94–96-amino acid-long N-terminal propeptide, which acts as a strong inhibitor of the enzymes, thereby maintaining their zymogen state. The propeptide consists of an inhibitory globular domain linked through an α-helical connecting segment (helix α3) to the enzyme core (Fig. 1). Seminal studies on the activation mechanism of bovine, porcine, rat, and human procarboxypeptidases elucidated that activation is initiated by tryptic cleavage at the C terminus of the connecting segment, which destabilizes helix α3 and leads to the dissociation of the inhibitory

* This work was supported, in whole or in part, by National Institutes of Health Grants R01 DK082412, R01 DK082412-S2 (American Recovery and Reinvestment Act), R01 DK058088 (to M. S.-T.), R01 AI44070 (to J. S.), P41 RR010888 (to C. E. C.), S10 RR020946 (to J. Zaia). This work was also supported by a scholarship from the Rosztoczy Foundation (to M. B.).

[S] The on-line version of this article (available at http://www.jbc.org) contains supplemental "Experimental Procedures," Tables S1–S5, and Fig. S1.

[1] Both authors contributed equally to this work.

[2] To whom correspondence should be addressed: 72 East Concord St., Evans-433, Boston, MA 02118. Tel.: 617-414-1070; Fax: 617-414-1041; E-mail: miklos@bu.edu.

[3] The abbreviations used are: CTRC, chymotrypsin C; CPA, carboxypeptidase A.

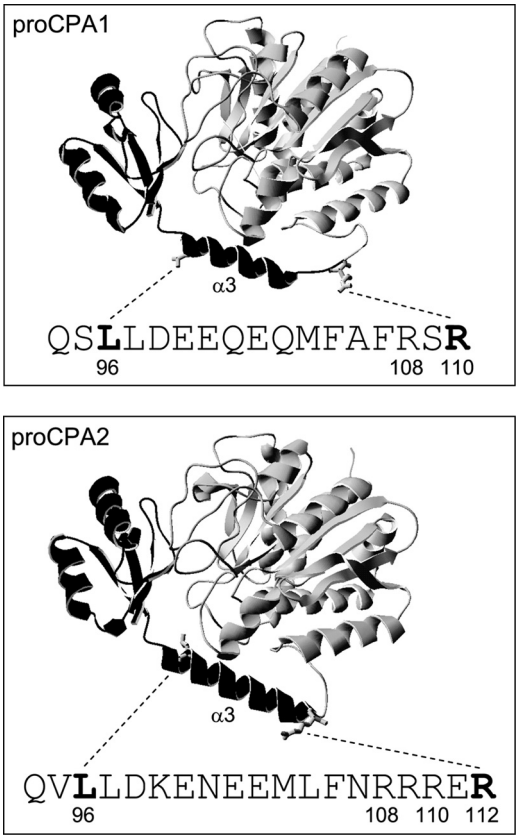

FIGURE 1. **Ribbon diagram of porcine proCPA1 (Protein Data Bank code 1PCA) and human proCPA2 (Protein Data Bank code 1AYE).** The propeptides are highlighted in *black*. The amino acid sequences of the α3 helices and the flanking tryptic activation sites in human proCPA1 and proCPA2 are indicated. The side chains for Leu^{96} (proCPA1 and proCPA2), Arg^{110} (proCPA1), and Arg^{112} (proCPA2) are shown. For clarity, the N-terminal amino acid residues have been removed, and the structures start with Gln^{24}. The image was rendered using DeepView/Swiss-PdbViewer (version 3.7).

domain (13–23). In the case of proCPA2 and proCPB, trypsin produced a monophasic activation curve, suggesting that trypsin alone was sufficient to cause propeptide dissociation and complete enzyme activation. In contrast, tryptic activation of proCPA1 was found biphasic, indicating that multiple proteolytic cleavages of the propeptide were necessary for the development of full CPA1 activity (13, 21). In porcine proCPA1, these cleavages occurred at a slow rate, and some were assumed to result from atypical trypsin activity at non-canonical sites (19). In addition to the critical role of trypsin, chymotrypsin and elastase were also shown in several studies to catalyze procarboxypeptidase activation to varying degrees; however, neither the mechanism nor cleavage sites involved in these alternative activation pathways have been clarified (16, 17, 22, 24). To date, no convincing attempt has been made to reconcile all biochemical data and define the likely physiological mechanism of procarboxypeptidase activation in the gut. Here, we describe that CTRC is a potent co-activator of human proCPA1 and proCPA2, as it facilitates dissociation of the propeptide and thereby increases carboxypeptidase activity by almost an order of magnitude. CTRC exerts its effect by proteolyzing the α-helical connecting segment of the propeptide, which becomes accessible only after tryptic activation. Because other human pancreatic proteases are much less effective at promoting procarboxypeptidase activation, CTRC emerges as a novel physiological co-activator of human proCPA1 and proCPA2.

EXPERIMENTAL PROCEDURES

Materials—Cell culture media and a Lipofectamine 2000 transfection reagent were obtained from Invitrogen. Carboxypeptidase substrates *N*-[4-methoxyphenylazoformyl]-L-phenylalanine and *N*-[4-methoxyphenylazoformyl)-L-arginine were purchased from Bachem (Torrance, CA). Human cationic trypsinogen (PRSS1) and proelastase 2A (ELA2A) were expressed in *Escherichia coli* and purified by ecotin affinity chromatography as described (25–28). Trypsinogen was activated to trypsin with human enteropeptidase (R&D Systems, Minneapolis, MN). Human CTRC, chymotrypsinogen B1 (CTRB1), chymotrypsinogen B2 (CTRB2), chymotrypsin-like enzyme-1 precursor (CTRL1), proelastase 3A (ELA3A), and proelastase 3B (ELA3B) were expressed in HEK 293T cells and purified from the conditioned medium by ecotin affinity chromatography (9, 28). CTRC, CTRL1, and ELA3B were purified as zymogens, whereas CTRB1, CTRB2, and ELA3A were purified after activation with trypsin. Human SPINK1 (serine protease inhibitor Kazal type 1) was expressed in HEK 293T cells and purified on a bovine trypsin affinity column (29). Chymotrypsinogens and proelastases were activated with immobilized bovine trypsin (Pierce; Thermo Fisher Scientific), and the trypsin-containing beads were removed by centrifugation. Protease concentrations were determined by active site titration with ecotin. Ecotin was expressed in *E. coli* and purified as described previously (30, 31).

Nomenclature—Amino acid residues were numbered starting with the initiator methionine of the primary translation product; according to the recommendations of the Human Genome Variation Society. The open reading frame of the human preproCPA2 contains two methionines at its N terminus (Met-Ala-Met-Arg-). Experimental evidence as to which methionine is used for translation initiation is lacking. Alignment with other mammalian CPA2 preproenzymes indicates that only the second methionine is conserved. Therefore, we arbitrarily designated the second methionine as the first amino acid residue of human preproCPA2.

Plasmid Construction and Mutagenesis—The cDNA for human preproCPA1 was amplified by PCR from IMAGE clone 3949850 (GenBank™ accession no. BC005279) using the CPA1-XhoI sense primer (5′-TTT AAA CTC GAG ACC TTC CCT CCC GGC AGC AGC ATG-3′ (where the XhoI site is underlined)) and the CPA1-BamHI antisense primer (5′-TTT AAA GGA TCC GCA AGC CCC AGG ATT CTG TTC CTG-3′ (where the BamHI site is underlined)). The PCR product was digested with XhoI and BamHI and subcloned into the pcDNA3.1(−) vector. The cDNA for human preproCPA2 was amplified by PCR from IMAGE clone 3950117 (GenBank™ accession no. BC014571) using the CPA2-NheI sense primer (5′-AAA TTT GCT AGC ACT CCA GGA AAA CCC ATG GCC ATG AGG-3′ (where the NheI site is underlined)) and the CPA2-EcoRI antisense primer (5′-AAA TTT GAA TTC AAA CCA AAG AGA TTT TAA TGG CTC

TTG-3′ (where the EcoRI site is underlined)). The PCR product was digested with NheI and EcoRI and subcloned into the pcDNA3.1(−) vector. The cDNA for human preproCPB1 was amplified by PCR from IMAGE clone 4422620 (GenBank™ accession no. BC015338) using the CPB1-XhoI sense primer (5′-AAA TTT CTC GAG TCA GAC ACA ATG TTG GCA CTC TTG GTT CTG GTG-3′ (where the XhoI site is underlined)) and the CPB1-BamHI antisense primer (5′-AAA TTT GGA TCC TCT CAA CTA GTA CAG GTG TTC CAG GAC GTA-3′ (where the BamHI site is underlined)). The PCR product was digested with XhoI and BamHI and subcloned into the pcDNA3.1(−) vector. Construction of pcDNA3.1(−) expression plasmids harboring the human CTRC; CTRB1; and CTRB2, ELA3A, ELA3B, and SPINK1 cDNAs was reported previously (9, 29). The cDNA for human CTRL1 precursor was PCR-amplified from IMAGE clone 5748224 (GenBank™ accession no. BC039716) with the CTRL1 EcoRI sense primer (5′-AAA TTT GAA TTC TCT GCC ACG ATG TTG CTG CTC AGC CTG-3′ (where the EcoRI site is underlined)) and CTRL1 BamHI antisense primer (5′-AAA TTT GGA TCC GTG AGC TCA GTT GTA GGC TAT GAC CTG-3′ (where the BamHI site is underlined)). The PCR product was digested with EcoRI and BamHI and subcloned into the pcDNA3.1(−) vector. The pTrapT7 bacterial expression plasmids harboring the human PRSS1 and ELA2A cDNAs were described earlier (25–27). Missense mutations in proCPA1 and proCPA2 were generated by overlap extension PCR mutagenesis and cloned in the appropriate expression plasmids.

Expression and Purification of Human ProCPA1, ProCPA2, and ProCPB1—HEK 293T cells were grown in DMEM with 10% FBS, and 4 mM L-glutamine in 75 cm^2 flasks to 95% confluence. Transfections were carried out using 30 μg of plasmid DNA and 75 μl of Lipofectamine 2000 reagent. After 16–20 h, cells were washed with Opti-MEM medium and covered with 20 ml of the same medium. Conditioned media were harvested after a 48-h incubation; replaced with 20 ml of fresh Opti-MEM and harvested again at 96 h. Conditioned media were dialyzed against 20 mM Tris-HCl (pH 8.0) and loaded directly onto a MonoQ column through the pump of a Pharmacia FPLC system. The column was developed with a NaCl gradient (0–0.5 M over 30 min at a flow rate of 1 ml/min). Fractions (1 ml) were collected and analyzed by SDS-PAGE and Coomassie Blue staining. The purest fractions (>90%) were used for experiments. Concentrations of the purified zymogen solutions were estimated from their ultraviolet absorbance at 280 nm, using extinction coefficients calculated with the web-based ProtParam tool.

Measurement of Carboxypeptidase Activity—CPA1 and CPA2 activity were determined using the *N*-[4-methoxyphenylazoformyl]-L-phenylalanine substrate at 60 μM final concentration (32). The assay mix contained 4 μl of CPA1/CPA2 enzyme (80 nM, final concentration), 86 μl of assay buffer (0.1 M Tris-HCl (pH 8.0) containing 1 mM $CaCl_2$ and 0.05% Tween 20) and 10 μl of 0.6 mM substrate dissolved in assay buffer. CPB1 activity was measured with *N*-[4-methoxyphenylazoformyl)-L-arginine under the same conditions (33). The decrease in absorbance was followed at 350 nm for 2 min in a SPECTRAmax Plus 384 microplate reader (Molecular Devices, Sunnyvale, CA). Rates of substrate consumption obtained in $mOD \cdot min^{-1}$ units (OD, optical density) were converted to $nM \cdot s^{-1}$ values using an extinction coefficient of 19,000 M^{-1} cm^{-1} corrected for the shorter path length of the microplate wells. Note that addition of $ZnCl_2$ (100 μM concentration) had no effect on the enzyme activity; therefore, it was omitted from the routine assay conditions.

Mass Spectrometry—Digestion reactions were stopped by adding 0.17% TFA (final concentration) and stored frozen. Prior to mass spectrometry, samples were desalted by micro solid-phase extraction using C4 ZipTips (Millipore, Billerica, MA). Briefly, C4 ZipTips were wetted with 80% acetonitrile and then equilibrated with 2% acetonitrile and 0.1% TFA. Proteins were bound to the resin by pipetting the samples through the tips several times, and the tips were washed with 2% acetonitrile and 0.1% TFA by pipetting this solution through the tip twice. Proteins were eluted with 10 μl 80% acetonitrile into Eppendorf tubes and transferred to 96-well plates (Advion, Ithaca, NY). High resolution mass spectra were acquired with direct infusion at a flow rate of 10 μl/min on a LTQ-Orbitrap™ hybrid mass spectrometer (Thermo Fisher Scientific) equipped with a TriVersa NanoMate ion source (Advion). Electrospray ionization was carried out at 1.7 kV using the NanoMate, with the LTQ heated capillary set to 150 °C. Mass spectra were acquired in the positive ion mode over the range m/z 300–2000 at a resolution of 60,000 (~1 mass spectrum/s). Mass accuracy after internal calibration was within 4 ppm. Data acquisition and analysis were performed using XCalibur software (Thermo Fisher Scientific). Experimental mass values were assigned to specific peptide sequences by PAWS software (Genomic Solutions, Holliston, MA).

RESULTS

Expression and Purification of Human ProCPA1 and ProCPA2—Human proCPA1 and proCPA2 were expressed in transiently transfected HEK 293T cells and purified from the conditioned medium as described under "Experimental Procedures." N-terminal sequencing of the mature zymogens yielded homogeneous sequences of Lys-Glu-Asp-Phe-Val for proCPA1 and Leu-Glu-Thr-Phe-Val for proCPA2, which corresponded to the N termini expected after removal of the secretory signal peptide (34, 35). Catalytic parameters were determined for the fully activated CPA1/CPA2 enzymes on the *N*-[4-methoxyphenylazoformyl]-L-phenylalanine substrate (supplemental Table S1). The k_{cat}/K_m values were comparable with or higher than those reported in the literature for native or recombinant human CPA1/CPA2 using small substrates (36–38).

Activation of Human ProCPA1 and ProCPA2 with Trypsin—Procarboxypeptidases (2 μM concentration) were incubated with human cationic trypsin (100 nM concentration), and the digestion products were visualized by SDS-PAGE. As shown in Fig. 2, trypsin converted the zymogen bands to a carboxypeptidase band and a smaller band (~12 kDa) corresponding to the released N-terminal propeptide. The reaction was nearly complete within 5 min, and both bands appeared

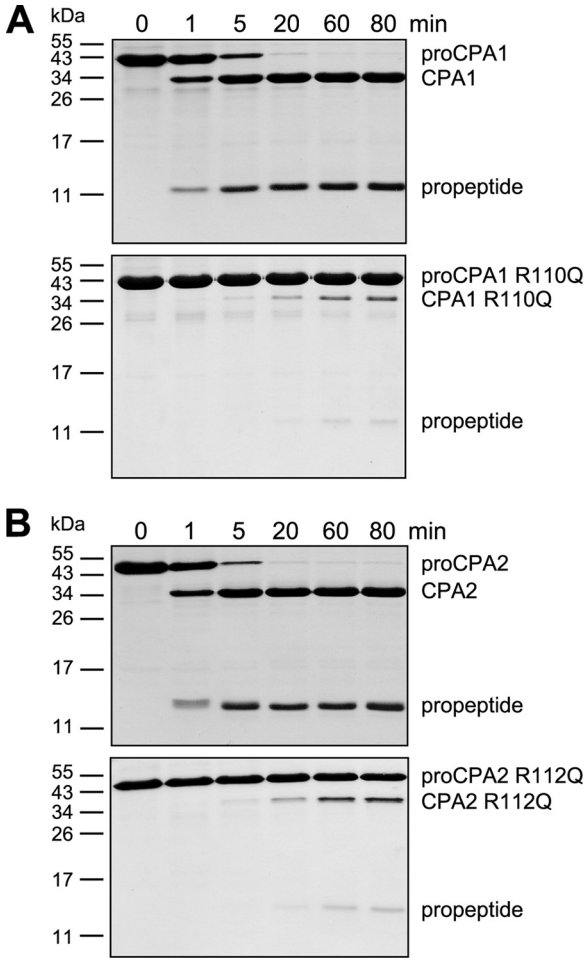

FIGURE 2. **Activation of proCPA1 (*A*), proCPA2 (*B*), the R110Q proCPA1 mutant (*A*), and the R112Q proCPA2 mutant (*B*) by trypsin.** Carboxypeptidase zymogens were incubated at 2 μM concentration with 100 nM human cationic trypsin at 37 °C in 20 mM Tris-HCl (pH 8.0) and 50 mM NaCl (final concentrations) in 100 μl final volume. At the indicated times, samples were precipitated with 10% trichloroacetic acid (final concentration) and analyzed by 15% SDS-PAGE and Coomassie blue staining. PageRuler prestained protein ladder was used to provide molecular mass markers (Fermentas, Glen Burnie, Maryland).

stable up to 80 min showing no signs of further degradation. N-terminal sequencing of the propeptides showed the same N termini as observed for the intact proenzymes, confirming that trypsin only cleaved at the C-terminal end of the propeptides. N-terminal sequencing of the CPA1 and CPA2 bands revealed homogeneous sequences of Ala-Arg-Ser-Thr-Asp and Ser-Gly-Asn-Phe-Asn, respectively, indicating that trypsin digested the Arg^{110}–Ala^{111} (proCPA1) and Arg^{112}–Ser^{113} (proCPA2) peptide bonds, known sites of tryptic activation (19, 23). To confirm the importance of these sites, Arg^{110} in proCPA1 and Arg^{112} in proCPA2 were mutated to Gln. As expected, these mutations dramatically reduced the rate of activation of both proenzymes by trypsin (Fig. 2).

Mass spectrometry of the CPA1/CPA2 propeptides, on the other hand, showed that the C-terminal amino acid after a 5-min trypsin activation was mainly Arg^{108}, consistent with tryptic cleavages of the Arg^{108}–Ser^{109} (proCPA1) and Arg^{108}–Arg^{109} (proCPA2) peptide bonds (supplemental Tables S2–S4). Propeptide forms ending in Arg^{110} (CPA1, CPA2) and Arg^{112} (CPA2) were also detected in lower amounts. Taken together with the N-terminal sequencing results (see above) and considering the protective effects of the R110Q (proCPA1) and R112Q (proCPA2) mutations, these observations suggest that trypsin acts in a sequential manner. First, it cleaves proCPA1 after Arg^{110}, followed by cleavage after Arg^{108}. In proCPA2, trypsin cleaves first after Arg^{112} and subsequently at Arg^{110} and Arg^{108}, in agreement with previously published data (23). Thus, trypsin removes two amino acids (Ser^{109}–Arg^{110}) from proCPA1 and four amino acids (Arg^{109}–Arg^{110}-Glu^{111}–Arg^{112}) from proCPA2 and generates stable, 92-amino acid-long propeptides from both human proenzymes (Fig. 1). Note that in proCPA2 helix α3 of the connecting segment is longer by a turn than in proCPA1; however, the α3 helices in the two proenzymes are trimmed to the same length as a result of tryptic activation.

Activity of Trypsin-activated CPA1 and CPA2 Is Markedly Increased by CTRC—Activation of proCPA1 or proCPA2 with human cationic trypsin resulted in the rapid appearance of carboxypeptidase activity, which reached a plateau at ~10 min and remained stable afterward (Fig. 3). Addition of relatively low concentrations of CTRC (50 nM) to trypsin-activated CPA1 or CPA2 caused a sudden and dramatic increase in carboxypeptidase activity, which was 8–10-fold higher than the activity obtained after trypsin-mediated activation alone (Fig. 3). Incubation of proCPA1 or proCPA2 with CTRC alone yielded no measurable carboxypeptidase activity, indicating that CTRC-mediated activation was dependent on prior tryptic activation of the carboxypeptidase zymogens. As expected, mutation of the catalytic serine 216 to alanine in CTRC abolished the activating effect of CTRC (data not shown). The observations suggest that trypsin-mediated activation of proCPA1 or proCPA2 does not result in complete dissociation of the inhibitory propeptide and subsequent cleavage(s) by CTRC are required for the complete elimination of inhibition and development of full carboxypeptidase activity. CTRC had no effect on the activity of CPB1 activated with trypsin (data not shown).

Trypsin-processed Propeptides Are Tight Binding Inhibitors of CPA1/CPA2—The partial (~10%) activity of trypsin-activated proCPA1/proCPA2 suggests that the trypsin-severed propeptide is still bound to the enzyme; however, either its binding affinity is weakened resulting in partial dissociation, or the propeptide underwent a conformational change partially exposing the active site. To distinguish between these two scenarios, we measured the concentration dependence of enzyme activity of trypsin-activated proCPA1/proCPA2. If the 10% activity is due to a conformational change of the bound propeptide, the concentration-activity relationship should be linear. On the other hand, if the 10% activity is due to weakened binding and partial dissociation of the propeptide, the concentration-activity relationship would show a square-root function; in agreement with the law of mass action. The experimental data shown in Fig. 4 clearly supported the latter case. In contrast, the concentration-activity relationships for CPA1/CPA2 fully activated with trypsin and CTRC gave completely linear functions (supplemental Fig. S1). The equilibrium dissociation constants (K_D) for the bind-

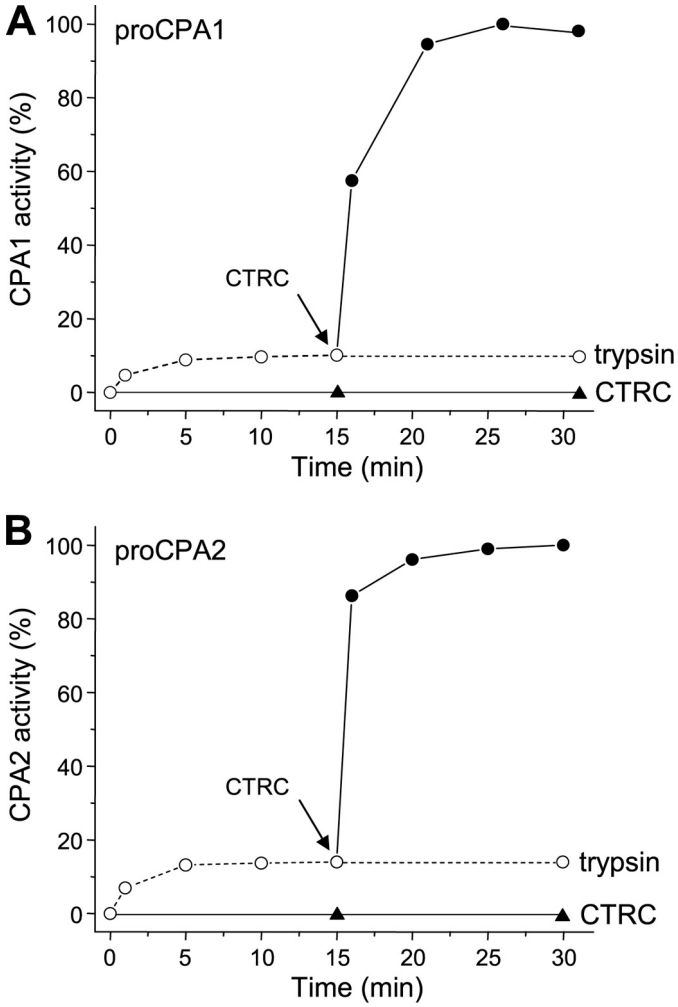

FIGURE 3. **Activation of proCPA1 (*A*) and proCPA2 (*B*) by trypsin and CTRC.** Carboxypeptidase zymogens were incubated at 2 μM concentration with 100 nM human cationic trypsin (*open circles*), 50 nM CTRC (*solid triangles*) or 50 nM CTRC added after 15 min preincubation with 100 nM trypsin (*solid circles*). Incubations were performed at 37 °C in 20 mM Tris-HCl (pH 8.0), 50 mM NaCl, and 0.05% Tween 20 (final concentrations) in 100 μl final volume. At the indicated times, carboxypeptidase activity was measured as described under "Experimental Procedures." The 100% activity levels corresponded to 450 nM·s^{-1} (CPA1) and 340 nM·s^{-1} (CPA2) substrate cleavage rates.

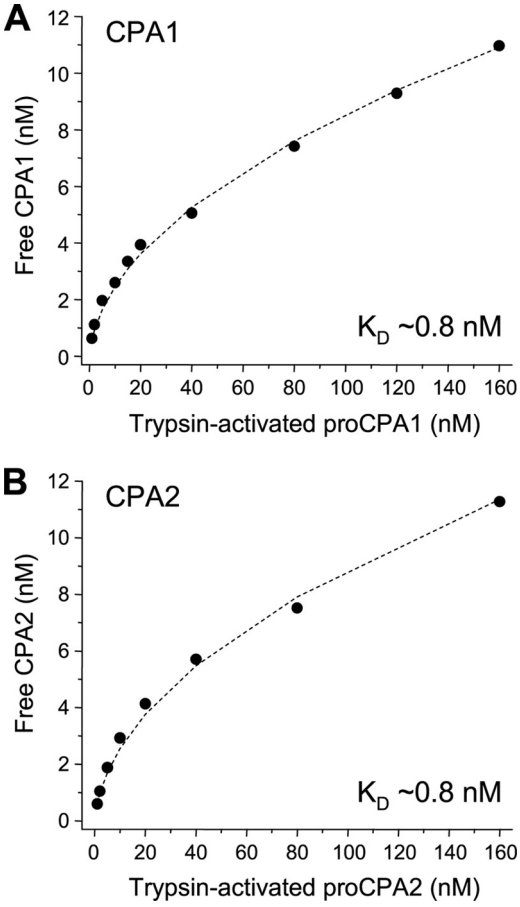

FIGURE 4. **Concentration dependence of carboxypeptidase activity of proCPA1 (*A*) and proCPA2 (*B*) activated with trypsin.** Carboxypeptidase zymogens were incubated at 2 μM concentration with 100 nM human cationic trypsin at 37 °C in 0.1 M Tris-HCl (pH 8.0), 50 mM NaCl, 1 mM $CaCl_2$, and 0.05% Tween 20 (final concentrations) in 100 μl final volume. After 30 min of incubation, activated proenzymes were diluted to the indicated concentrations with assay buffer (0.1 M Tris-HCl (pH 8.0), 1 mM $CaCl_2$, 0.05% Tween 20) and incubated for 10 min at 22 °C. Carboxypeptidase activity was then measured by adding 10 μl of *N*-[4-methoxyphenylazoformyl]-L-phenylalanine substrate to 60 μM final concentration, as described under "Experimental Procedures." Carboxypeptidase activities were converted to free CPA1/CPA2 concentrations by dividing the activity values with the slope of the linear concentration-activity plots of trypsin and CTRC activated CPA1/CPA2 shown in supplemental Fig. S1. Data points were fitted to the equation $y = (-K + \mathrm{sqrt}(K^2 + 4Kx))/2$, where K is the equilibrium dissociation constant. This equation is the positive solution to the $K = y^2/x - y$ quadratic equation, which expresses the law of mass action applied to the dissociation of carboxypeptidase and its propeptide. The variable x corresponds to the total concentration of trypsin-activated proCPA1/proCPA2 present in the reaction, and y is the concentration of free CPA1/CPA2 in equilibrium. The concentration of the inhibited CPA1/CPA2 complex in equilibrium is described by $x - y$.

ing of the CPA1/CPA2 propeptides were estimated from Fig. 4 as 0.8 nM.

CTRC Degrades Trypsin-processed CPA1/CPA2 Propeptides—CTRC alone did not cleave the intact proCPA1 and proCPA2 zymogens to any detectable extent, as judged by SDS-PAGE (data not shown). In contrast, addition of CTRC to trypsin-activated CPA1/CPA2 resulted in relatively rapid degradation of the propeptide (Fig. 5). Catalytically impaired carboxypeptidase variants were also produced by mutating Arg^{237} in CPA1 and Arg^{235} in CPA2 to Ala. Arg^{237} corresponds to Arg^{127} in the mature CPA1 enzyme; and mutation of this amino acid in rat CPA1 was previously shown to decrease catalytic activity by four orders of magnitude (39, 40). The trypsin-processed propeptides of the R237A proCPA1 and R235A proCPA2 mutants were also readily degraded by CTRC (Fig. 4), indicating that CPA1/CPA2 activity is not required for propeptide degradation.

To determine CTRC cleavage sites in the propeptides, the digestion product mixtures were analyzed by mass spectrometry. These efforts were hampered by the fact that CPA1/CPA2 removed C-terminal amino acids exposed by CTRC-mediated cleavages. Therefore, we first analyzed the catalytically impaired proCPA1 R237A and proCPA2 R235A mutants (supplemental Table S2). Second, Leu^{96}–Leu^{97} were replaced with Ile in this inactive background, and the resulting mutants L96I,L97I,R237A (proCPA1) and L96I,L97I,R235A (proCPA2) were tested (supplemental Table S3). Because CTRC cannot cleave after Ile, these mutants were expected to allow us to capture early cleavage intermedi-

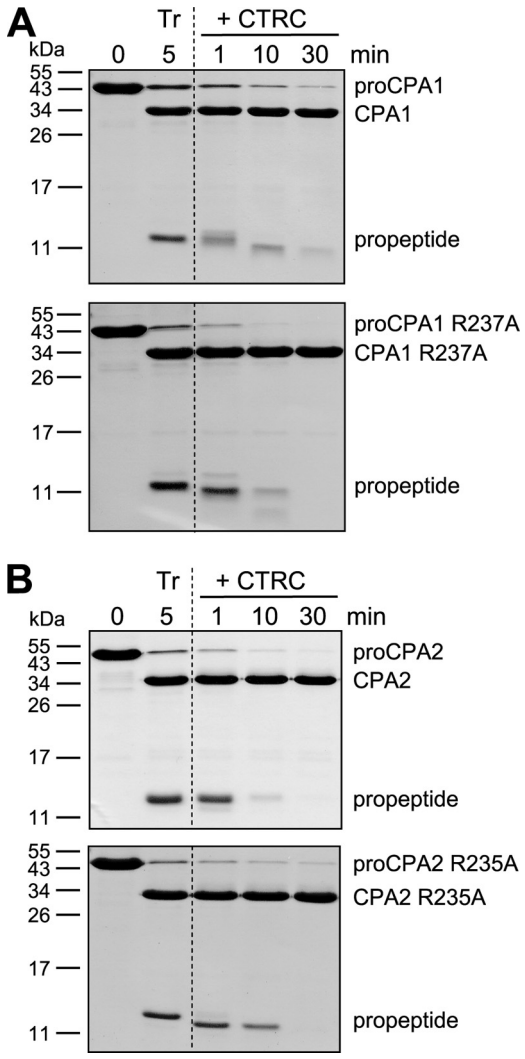

FIGURE 5. **Activation of proCPA1 (*A*), proCPA2 (*B*), the R237A proCPA1 mutant (*A*), and the R235A proCPA2 mutant (*B*) by trypsin (*Tr*) and CTRC.** Procarboxypeptidases were incubated at 2 μM concentration with 100 nM human cationic trypsin at 37 °C in 20 mM Tris-HCl (pH 8.0), 50 mM NaCl (final concentrations) in 100 μl final volume. After 5 min, 50 nM CTRC (final concentration) was added to the incubation reactions. At the indicated times, samples were precipitated with 10% trichloroacetic acid (final concentration) and analyzed by 15% SDS-PAGE and Coomassie Blue staining. PageRuler prestained protein ladder was used to provide molecular mass markers (Fermentas).

ates in the C-terminal half of helix α3. Finally, to estimate the contribution of CPA1/CPA2 activity to propeptide degradation, the wild-type proenzymes were studied (supplemental Table S4). Taken together, the results from these three data sets indicated that CTRC first cleaved within the C-terminal third of helix α3 (1 min), followed by cleavages at the N-terminal end of the helix (1 min, 10 min). These cleavages destabilized the globular inhibitory domain, which was then cleaved by CTRC and trypsin at multiple sites (10 min, 30 min). From comparison of the time course of propeptide degradation by CTRC and the development of carboxypeptidase activity (Fig. 3), it was apparent that degradation of helix α3 was sufficient to induce complete dissociation of the inhibitory propeptide. The location of the specific CTRC cleavage sites were determined as described in the following section.

After tryptic activation, CTRC first attacked peptide bonds located in the C-terminal third of helix α3 in both proCPA1 and proCPA2. CTRC cleaved the Phe^{105}–Ala^{106} and Gln^{103}–Met^{104} peptide bonds in proCPA1; and the Phe^{106}–Asn^{107} and Met^{104}–Leu^{105} peptide bonds in proCPA2, most likely in a sequential manner. The Met^{104}–Phe^{105} peptide bond in proCPA1 and the Leu^{105}–Phe^{106} peptide bond in proCPA2 were also cleaved at low but detectable levels. CPA1/CPA2 activity probably also contributed to the digestion of the propeptides by removing the C-terminal residues exposed by CTRC, although the exact cleavages could not be ascertained from the results.

The N-terminal end of helix α3 was cleaved first at the conserved Leu^{96}–Leu^{97} peptide bond in both proCPA1 and proCPA2. This was followed by cleavage of the Gln^{94}–Ser^{95} peptide bond in proCPA1. Digestion of the analogous Gln^{94}–Val^{95} peptide bond in proCPA2 was less significant. In proCPA1, Leu^{96} was removed by CPA1 after CTRC cleavage of the Leu^{96}–Leu^{97} peptide bond and Gln^{94} and Val^{93} were sequentially excised after CTRC cleavage of the Gln^{94}–Ser^{95} peptide bond. In proCPA2, Leu^{96} and Val^{95} were removed by CPA2 after CTRC cleavage of the Leu^{96}–Leu^{97} peptide bond.

At longer digestion times (10–30 min), several smaller peptides were detected, which were generated by a combination of chymotryptic and tryptic cleavages within the inhibitory domain of the propeptide. Thus, in proCPA1 cleavages were detected at the Leu^{26}–Arg^{27}, Arg^{27}–Ile^{28}, Gln^{37}–Lys^{38}, Leu^{48}–Gln^{49}, Leu^{50}–Asp^{51}, Arg^{54}–Gly^{55}, Gln^{73}–Ala^{74}, Lys^{76}–Ile^{77}, and Phe^{78}–Leu^{79} peptide bonds, whereas in proCPA2, peptide bonds Leu^{26}–Glu^{27}, Lys^{37}–Asn^{38}, Leu^{39}–Leu^{40}, Leu^{40}–Gln^{41}, Leu^{48}–Gln^{49}, Leu^{50}–Asp^{51}, Lys^{54}–Ser^{55}, Phe^{69}–Val^{70}, Lys^{76}–Val^{77}, and Phe^{78}–Leu^{79} were cleaved (supplemental Table S2).

Cleavage of Conserved Leu^{96}–Leu^{97} Peptide Bond Is Required for Full CPA1/CPA2 Activation—To test whether complete degradation of helix α3 is necessary for the development of full CPA1/CPA2 activity, amino acids Leu^{96}–Leu^{97} were mutated to Ile (mutant L96I,L97I) in proCPA1 and proCPA2. In these mutants, CTRC is expected to cleave at the C-terminal half of helix α3; however, cleavage at the N terminus of helix α3 would be inhibited, as CTRC cannot digest isoleucyl peptide bonds. Addition of CTRC to the trypsin-activated L96I,L97I proCPA1 mutant resulted in a biphasic activation pattern. First, carboxypeptidase activity rapidly increased to ~30% of the potential maximum, followed by a slow increase to ~50% during the time course studied (Fig. 6). In the case of the L96I, L97I proCPA2 mutant a similar biphasic pattern was evident; the rapid phase resulted in about 15% activity, which slowly increased to ~35%. These observations clearly indicate that cleavage in the C-terminal part of helix α3 of the propeptide results in partial CPA1/CPA2 activation only and cleavage of the conserved Leu^{96}–Leu^{97} peptide bond at the N terminus of helix α3 is required for full activation.

CTRC Is Physiological Co-activator of ProCPA1 and ProCPA2—The robust procarboxypeptidase activating action of CTRC was unique among human pancreatic proteases, suggesting that CTRC is the physiological co-activator of proCPA1 and proCPA2. Thus, incubation with 50 nM concen-

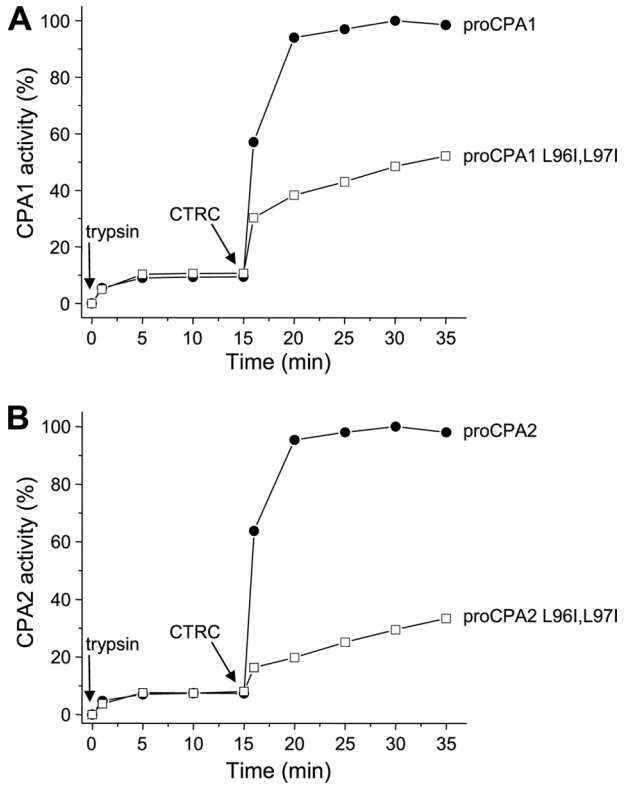

FIGURE 6. **Activation of the L96I,L97I proCPA1 (*A*) and L96I,L97I proCPA2 (*B*) mutants by trypsin and CTRC.** Procarboxypeptidase mutants and wild-type control were incubated at 2 μM concentration with 100 nM human cationic trypsin for 15 min followed by 50 nM CTRC (final concentrations). Incubations were performed at 37 °C in 20 mM Tris-HCl (pH 8.0), 50 mM NaCl and 0.05% Tween 20 (final concentrations) in 100 μl final volume. At the indicated times, carboxypeptidase activity was measured as described under "Experimental Procedures." The 100% activity levels corresponded to 450 nM·s^{-1} (CPA1) and 340 nM·s^{-1} (CPA2) substrate cleavage rates.

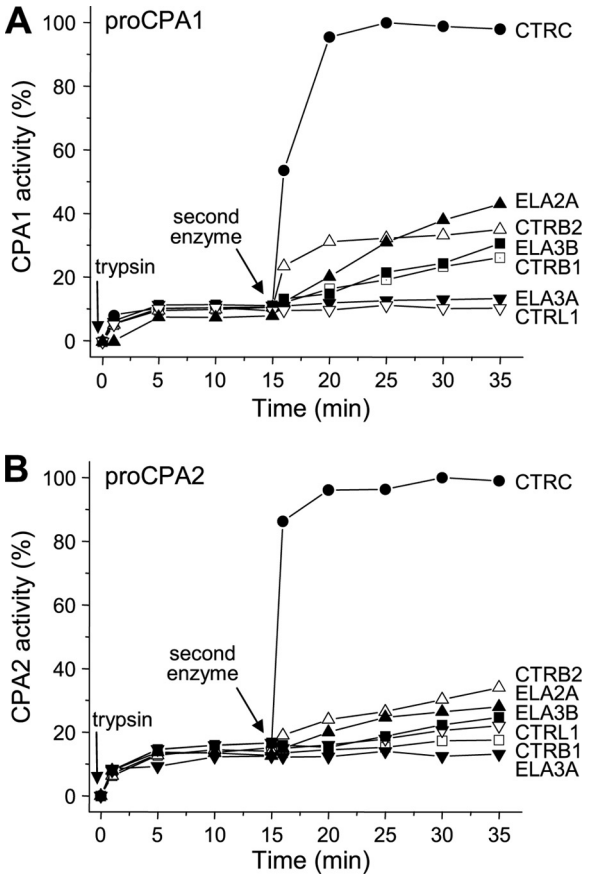

FIGURE 7. **Activation of proCPA1 (*A*) and proCPA2 (*B*) by trypsin and human pancreatic proteases.** Carboxypeptidase zymogens were incubated at 2 μM concentration with 100 nM human cationic trypsin for 15 min followed by 50 nM of the indicated proteases (final concentrations). Incubations were performed at 37 °C in 20 mM Tris-HCl (pH 8.0), 50 mM NaCl, and 0.05% Tween 20 (final concentrations) in 100 μl final volume. At given times, carboxypeptidase activity was measured as described under "Experimental Procedures." The 100% activity levels corresponded to 450 nM·s^{-1} (CPA1) and 340 nM·s^{-1} (CPA2) substrate cleavage rates.

tration of elastase 2A (ELA2A), elastase 3A (ELA3A), elastase 3B (ELA3B), chymotrypsin B1 (CTRB1); chymotrypsin B2 (CTRB2) or chymotrypsin-like enzyme-1 (CTRL1) resulted in minimal or limited further activation of trypsin-activated CPA1 and CPA2 (Fig. 7). Interestingly, chymotrypsin B2 (CTRB2) activated the trypsin-processed CPA1 relatively rapidly, but the maximal carboxypeptidase activity was only ~30% of that achieved by CTRC. Mass spectrometry indicated that CTRB2 cleaved the trypsin-processed CPA1 propeptide at the Phe^{105}–Ala^{106} peptide bond (data not shown). These observations also provided independent confirmation that proteolytic cleavage in the C-terminal third of helix α3 can induce only partial CPA1 activation, as described in the previous section.

Trypsin-independent Activation of ProCPA1 by CTRB2—We found that CTRB2 at 100–200 nM concentration could slowly cleave the intact proCPA1 propeptide and thereby elicit partial CPA1 activation (~30% of potential maximum), even without prior activation with trypsin (Fig. 8). However, relative to the trypsin-mediated propeptide cleavage, this reaction proceeded at least 10-fold slower suggesting that it is unlikely to be of physiological significance. Addition of CTRC to the CTRB2-activated CPA1 resulted in full CPA1 activity (Fig. 8). CTRB2 cleaved the Phe^{105}–Ala^{106} and Phe^{107}–Arg^{108} peptide bonds in the C-terminal half of helix α3, in an unspecified order, as evidenced by mass spectrometry (C-terminal residue of cleaved propeptide was Phe^{105}; data not shown) and N-terminal sequencing (N terminus of CPA1 was Arg^{108}).

DISCUSSION

The present study offers compelling evidence that the human A-type procarboxypeptidases are activated by the sequential action of trypsin and CTRC. The activation mechanism of proCPA1 and proCPA2 can be arbitrarily divided into four phases. (i) A series of trypsin-mediated cleavages at the C terminus of the propeptide, which result in the removal of two amino acid residues (Ser^{109}–Arg^{110} in proCPA1) or four amino acid residues (Arg^{109}–Arg^{110}–Glu^{111}–Arg^{112} in proCPA2) and generate a stable 92-amino acid-long propeptide. This propeptide is still inhibitory; however, binding is already compromised as evidenced by the appearance of ~10% carboxypeptidase activity. (ii) The propeptide is cleaved by CTRC in the C-terminal third of helix α3 at multiple adjacent sites. Amino acids exposed by CTRC cleavages may be trimmed by CPA1/CPA2 action. The inhibitory potential of the propeptide is further reduced by these cleavages,

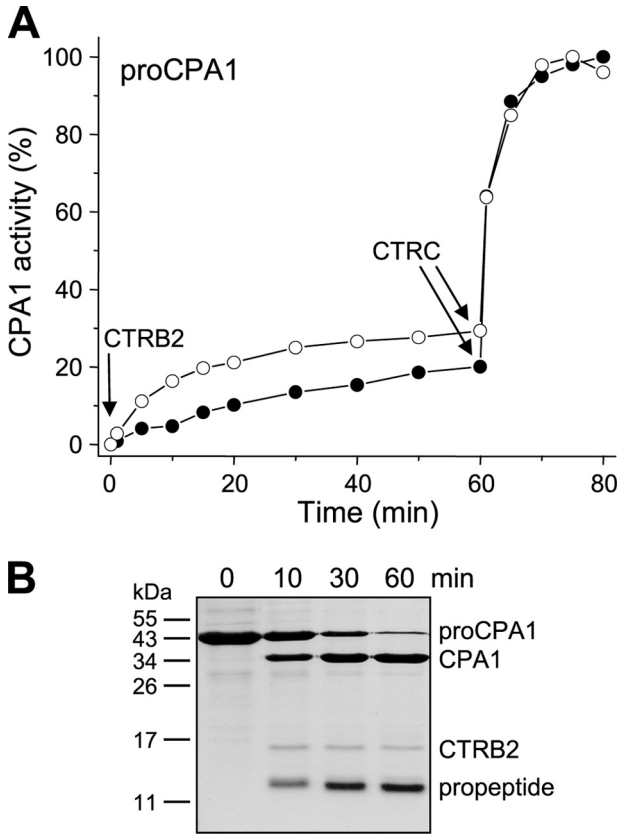

FIGURE 8. **Activation of proCPA1 by CTRB2.** *A*, procarboxypeptidase A1 was incubated at 2 μM concentration with 100 nM (*solid symbols*) or 200 nM (*open symbols*) CTRB2 for 60 min followed by 50 nM CTRC (final concentrations). Incubations were performed at 37 °C in 20 mM Tris-HCl (pH 8.0), 50 mM NaCl, and 0.05% Tween 20 (final concentrations) in 100 μl final volume. Reactions also contained human SPINK1 at 70 nM concentration to inhibit any unforeseen trypsin contamination. At given times, carboxypeptidase activity was measured as described under "Experimental Procedures." The 100% activity level corresponded to 450 nM·s^{-1} substrate cleavage rate. *B*, alternatively, reactions were precipitated with 10% trichloroacetic acid (final concentration) and analyzed by 15% SDS-PAGE and Coomassie Blue staining. The experiment shown was performed with 100 nM CTRB2 concentration. Note that CTRB2 is physiologically autolyzed at the Tyr^{164}–Asn^{165} peptide bond generating 14-kDa and 10.4-kDa fragments on reducing gels. The larger fragment is clearly visible on the gel, whereas the smaller fragment can be observed as a faint band above the CPA1 propeptide. A PageRuler prestained protein ladder was used to provide molecular mass markers (Fermentas).

which results in the development of ~30% (CPA1) and 15% (CPA2) of the potential maximal carboxypeptidase activity. (iii) Helix α3 is cleaved by CTRC at its N terminus at the conserved Leu^{96}–Leu^{97} peptide bond. Leu^{96} is removed by CPA1/CPA2 activity, and the CPA2 propeptide is further shortened by excision of Val^{95}, whereas in proCPA1, Ser^{95} is digested inefficiently. Instead, CTRC cleaves the Gln^{94}–Ser^{95} peptide bond in proCPA1. At this stage, helix α3 of the propeptide is fully degraded, and CPA1/CPA2 are relieved of inhibition, resulting in full carboxypeptidase activity. (iv) CTRC and trypsin digest the dissociated globular domain of the propeptide to small peptides. In the physiological setting, other proteases are likely to contribute to this last phase.

The activation mechanism described above conforms to the general principles of the previously proposed activation pathways (13, 19–21). Thus, trypsin cleavage at the C-terminal end of the propeptide is an obligatory initiating event in proCPA1/proCPA2 activation, which destabilizes helix α3 and renders it susceptible to further proteolytic attack. Previous studies on porcine CPA suggested that these were catalyzed by slow and sometimes atypical tryptic cleavages (19); however, here, we clearly show that the trypsin-cleaved propeptide is highly stable and efficient proteolysis of helix α3 can be catalyzed by CTRC only. Although CPA1 and CPA2 contribute to the degradation of their own propeptides, this activity does not seem essential as the propeptides of catalytically impaired CPA1/CPA2 mutants are also completely degraded by trypsin and CTRC (see Fig. 5). In contrast to published reports suggesting that proCPA2 is activated by trypsin alone (13, 18, 21–23), we found that the activation mechanism of proCPA1 and proCPA2 are highly similar and dependent on both trypsin and CTRC. On the other hand, activation of proCPB1 does not require CTRC and most likely depends on trypsin only, as described previously (13, 18, 20–21, 41).

Alignment of rat, mouse, bovine, porcine, and human CPA1/CPA2 propeptides indicates that Leu^{96}–Leu^{97} is completely conserved and CTRC-sensitive sites in the C-terminal half of helix α3 are also present in these species. Therefore, it is likely that the activation mechanism identified in this study is generally applicable to all mammalian procarboxypeptidases of the A-type. It is intriguing to note that CTRC is found in complex with CPA and proproteinase E (which corresponds to ELA3B in humans) in ruminants, including the cow, goat, and sheep (5–7). It would seem reasonable to speculate that in these species CPA activation is further enhanced by steric proximity of CPA and its co-activator CTRC. Surprisingly, however, it has been reported that CPA is activated by trypsin very slowly in the bovine ternary complex, even though CTRC activation was relatively rapid, indicating that the CPA propeptide is poorly accessible to CTRC in the complex (15).

Previous studies suggested that chymotrypsin and elastase might activate procarboxypeptidases in the absence of trypsin (16, 17, 22, 24). We found, however, that human elastases and chymotrypsins, other than CTRC, activated proCPA1/proCPA2 poorly, even after activation with trypsin (see Fig. 7). The only exception was CTRB2, which cleaved the intact CPA1 propeptide and induced partial (~30%) activation of proCPA1 but at a rate that was by an order of magnitude slower than trypsin-catalyzed proCPA1 activation. Therefore, CTRB2 is unlikely to play a significant role in physiological proCPA1/proCPA2 activation.

Finally, the results presented here confirm and extend the notion that CTRC is a unique digestive protease which, beyond its digestive function, also plays an important role in regulating the activation and degradation of other digestive enzymes, trypsinogens (8, 9), and procarboxypeptidases in particular. Other human pancreatic chymotrypsins and elastases are ineffective at cleaving the CTRC-specific regulatory sites. The specificity of CTRC can be partly explained by its affinity for leucyl peptide bonds. Furthermore, alignment of sequences flanking the regulatory cleavage sites in trypsinogen and the Leu^{96}–Leu^{97} peptide bond in proCPA1/proCPA2 reveals a clustering of acidic amino acid residues on the prime

side of the scissile peptide bonds (supplemental Table S5). It appears likely that (some of) these acidic residues might govern CTRC recognition and impart high specificity to CTRC-mediated cleavages.

Acknowledgments—We thank Gábor Pál (Department of Biochemistry, Eötvös University, Budapest, Hungary) for helpful discussions and critical reading of the manuscript. Protein sequencing was performed by David McCourt (Midwest Analytical, Inc., St. Louis, MO).

REFERENCES

1. Folk, J. E., and Schirmer, E. W. (1965) *J. Biol. Chem.* **240,** 181–192
2. Folk, J. E., and Cole, P. W. (1965) *J. Biol. Chem.* **240,** 193–197
3. Keil-Dlouha, V., Puigserver, A., Marie, A., and Keil, B. (1972) *Biochim. Biophys. Acta* **276,** 531–535
4. Iio-Akama, K., Sasamoto, H., Miyazawa, K., Miura, S., and Tobita, T. (1985) *Biochim. Biophys. Acta* **831,** 249–256
5. Brown, J. R., Cox, D. J., Greenshields, R. N., Walsh, K. A., Yamasaki, M., and Neurath, H. (1961) *Proc. Natl. Acad. Sci. U.S.A.* **47,** 1554–1560
6. Kerfelec, B., Chapus, C., and Puigserver, A. (1985) *Eur. J. Biochem.* **151,** 515–519
7. Gomis-Rüth, F. X., Gómez, M., Bode, W., Huber, R., and Avilés, F. X. (1995) *EMBO J.* **14,** 4387–4394
8. Nemoda, Z., and Sahin-Tóth, M. (2006) *J. Biol. Chem.* **281,** 11879–11886
9. Szmola, R., and Sahin-Tóth, M. (2007) *Proc. Natl. Acad. Sci. U.S.A.* **104,** 11227–11232
10. Rosendahl, J., Witt, H., Szmola, R., Bhatia, E., Ozsvári, B., Landt, O., Schulz, H. U., Gress, T. M., Pfützer, R., Löhr, M., Kovacs, P., Blüher, M., Stumvoll, M., Choudhuri, G., Hegyi, P., te Morsche, R. H., Drenth, J. P., Truninger, K., Macek, M., Jr., Puhl, G., Witt, U., Schmidt, H., Büning, C., Ockenga, J., Kage, A., Groneberg, D. A., Nickel, R., Berg, T., Wiedenmann, B., Bödeker, H., Keim, V., Mössner, J., Teich, N., and Sahin-Tóth, M. (2008) *Nat. Genet.* **40,** 78–82
11. Masson, E., Chen, J. M., Scotet, V., Le Maréchal, C., and Férec, C. (2008) *Hum. Genet.* **123,** 83–91
12. Whitcomb, D. C., Gorry, M. C., Preston, R. A., Furey, W., Sossenheimer, M. J., Ulrich, C. D., Martin, S. P., Gates, L. K., Jr., Amann, S. T., Toskes, P. P., Liddle, R., McGrath, K., Uomo, G., Post, J. C., and Ehrlich, G. D. (1996) *Nat. Genet.* **14,** 141–145
13. Avilés, F. X., Vendrell, J., Guasch, A., Coll, M., and Huber, R. (1993) *Eur. J. Biochem.* **211,** 381–389
14. Vendrell, J., Querol, E., and Avilés, F. X. (2000) *Biochim. Biophys. Acta* **1477,** 284–298
15. Keller, P. J., Cohen, E., and Neurath, H. (1958) *J. Biol. Chem.* **230,** 905–915
16. Uren, J. R., and Neurath, H. (1972) *Biochemistry* **11,** 4483–4492
17. Chapus, C., Kerfelec, B., Foglizzo, E., and Bonicel, J. (1987) *Eur. J. Biochem.* **166,** 379–385
18. Pascual, R., Burgos, F. J., Salva, M., Soriano, F., Mendez, E., and Aviles, F. X. (1989) *Eur. J. Biochem.* **179,** 609–616
19. Vendrell, J., Cuchillo, C. M., and Avilés, F. X. (1990) *J. Biol. Chem.* **265,** 6949–6953
20. Guasch, A., Coll, M., Avilés, F. X., and Huber, R. (1992) *J. Mol. Biol.* **224,** 141–157
21. Vendrell, J., Guasch, A., Coll, M., Villegas, V., Billeter, M., Wider, G., Huber, R., Wüthrich, K., and Avilés, F. X. (1992) *Biol. Chem. Hoppe Seyler* **373,** 387–392
22. Oppezzo, O., Ventura, S., Bergman, T., Vendrell, J., Jörnvall, H., and Avilés, F. X. (1994) *Eur. J. Biochem.* **222,** 55–63
23. Reverter, D., Ventura, S., Villegas, V., Vendrell, J., and Avilés, F. X. (1998) *J. Biol. Chem.* **273,** 3535–3541
24. Lacko, A. G., and Neurath, H. (1970) *Biochemistry* **9,** 4680–4690
25. Sahin-Tóth, M. (2000) *J. Biol. Chem.* **275,** 22750–22755
26. Sahin-Tóth, M., and Tóth, M. (2000) *Biochem. Biophys. Res. Commun.* **278,** 286–289
27. Szepessy, E., and Sahin-Tóth, M. (2006) *Pancreatology* **6,** 117–122
28. Lengyel, Z., Pál, G., and Sahin-Tóth, M. (1998) *Protein Expr. Purif.* **12,** 291–294
29. Király, O., Boulling, A., Witt, H., Le Maréchal, C., Chen, J. M., Rosendahl, J., Battaggia, C., Wartmann, T., Sahin-Tóth, M., and Férec, C. (2007) *Hum. Mutat.* **28,** 469–476
30. Pál, G., Sprengel, G., Patthy, A., and Gráf, L. (1994) *FEBS Lett.* **342,** 57–60
31. Pál, G., Szilágyi, L., and Gráf, L. (1996) *FEBS Lett.* **385,** 165–170
32. Mock, W. L., Liu, Y., and Stanford, D. J. (1996) *Anal. Biochem.* **239,** 218–222
33. Mock, W. L., and Stanford, D. J. (2002) *Bioorg. Med. Chem. Lett.* **12,** 1193–1194
34. Catasús, L., Villegas, V., Pascual, R., Avilés, F. X., Wicker-Planquart, C., and Puigserver, A. (1992) *Biochem. J.* **287,** 299–303
35. Catasús, L., Vendrell, J., Avilés, F. X., Carreira, S., Puigserver, A., and Billeter, M. (1995) *J. Biol. Chem.* **270,** 6651–6657
36. Peterson, L. M., Sokolovsky, M., and Vallee, B. L. (1976) *Biochemistry* **15,** 2501–2508
37. Laethem, R. M., Blumenkopf, T. A., Cory, M., Elwell, L., Moxham, C. P., Ray, P. H., Walton, L. M., and Smith, G. K. (1996) *Arch. Biochem. Biophys.* **332,** 8–18
38. Reverter, D., García-Sáez, I., Catasús, L., Vendrell, J., Coll, M., and Avilés, F. X. (1997) *FEBS Lett.* **420,** 7–10
39. Phillips, M. A., Fletterick, R., and Rutter, W. J. (1990) *J. Biol. Chem.* **265,** 20692–20698
40. Phillips, M. A., Hedstrom, L., and Rutter, W. J. (1992) *Protein Sci.* **1,** 517–521
41. Villegas, V., Vendrell, J., and Avilés, X. (1995) *Protein Sci.* **4,** 1792–1800